Production of Highly Charged Ions in Neon Following Photoionization and Resonant Excitation

Yehia A. Lotfy

El-Minia University, Faculty of Science, Physics Department, 61111 El-Minia, Egypt

The final charge state distributions of ions are calculated after photoionization $1s \rightarrow \infty$, $2s \rightarrow \infty$ *and resonant excitation* $1s \rightarrow 3p$ *and* $2s \rightarrow 3p$ *in neon atoms. The calculation of vacancy cascades based on the simulation of radiative and non-radiative pathways to fill the inner-shell hole and spectator vacancies in atomic configurations. The charged ions at 1s hole state after photoionization mainly turns into* Ne^{2+} *and* Ne^{3+} *ions. In the1s hole situation, the doubly charged* Ne^{2+} *following photoionization are predominate, while in 2s hole situation the singly charged* Ne^{1+} *ions are the most abundant one. At 2s hole state after photoionization and resonant excitation, the charged* Ne^{1+} *predominate in the distributions. The consideration of electron shake off processes improves the results of final charge state distribution. The results of charge state distributions of ions after core hole production agree well with the experimental values.*

1. Introduction:

The inner-shell vacancy in ground state atom is formed leaving an ionic state, could be transferred into ground state via a cascade of successive radiative (x-ray) and non-radiative (Auger and Coster- Kronig) transitions. The cascades of these radiative and non-radiative transitions lead to the ejection of electrons and yield highly charged ions. Each Auger transition increases the charge of the ion by one, while radiative transition leaves the charge state unaltered. In the case of x-ray processes the vacancy moves to an outer shell under emission of characteristic x-rays, while for non-radiative transitions one electron from an outer shell fills up the inner-shell vacancy and another electron is ejected into continuum. In addition to the vacancy filling processes, there is an electron shake off process due to the change of core potential of the atom, which causes after inner-shell vacancy creation and through the filling processes.

The study of successive radiative (x-ray) and non-radiative (Auger and Coster- Kronig) transitions following inner-shell ionization and the highly charged ions which is connected with the cascades, is of interest in different fields of research such as solid state physics, plasma physics and astrophysics. The investigation of vacancy cascades is important for studying the storage of thermal multi-charged ions [1] and for the decomposition of large molecules following electron pick-up [2]. The study of post-collision interactions and relaxation processes in inner-shell ionization is usually performed by analysis of electrons or ions produced by successive radiative (x-ray) and non-radiative (Auger and Coster-Kronig) transitions. The structure and the dynamics (e.g. energies, transition probabilities, and electron correlation) of atoms and molecules are probed via Auger cascades production.

The readjustment of neon atom ionized in the *K* shell by x-ray has been measured with a coincidence time-of-flight mass spectrometer [3]. However, in the case of neon atoms (Nobel gas) the highly charged ions producing after inner shell ionization are not destroyed and can be observed experimentally. The relative abundance have been measured for the ions that are formed as the result of atomic adjustment to vacancies in the *K* and *L* shell of rare gases atoms [4-8]. The charge state distribution of ions result from de-excitation decay of inner-shell vacancies was measured by sweeping the photo energy across the ionization threshold [9-12] using synchrotron radiation and time-of light spectrometer.

There are two major theoretical studies to calculate the highly charged ions after inner-shell ionization in atoms. The first one is based on straightforward construction of the vacancy cascades accompanied with trees of radiative and non-radiative transitions [13-16]. The second method is based on simulation of all possible radiative and non-radiative pathways, which fill the inner-shell vacancies in atoms [17-21].

In the present work, the final charge state distributions following *1s* and *2s* photoionization and resonant excitation are calculated. The vacancy cascades are based on simulation of radiative, non-radiative transitions pathway to fill the inner-shell vacancies and electron shake off processes in neon atoms. The radiative and non-radiative transitions are calculated for single ionized neon. The radiative and non-radiative transitions for multi-ionized (several vacancies) are obtained using the scaling procedure that is dependent on the occupation number of electrons in atomic configurations through the vacancy cascade propagation. The results of final charge state are compared with theoretical and experimental values.

2. Method of calculation:

A radiative (x-ray) and non-radiative (Auger and Coster-Kronig) states are created by inner-shell ionization in atoms. Inner- shell (core) electrons are meant all electrons except the outermost electrons. The production of inner-shell vacancy in the target atom A is performed by photoionization

$$A + h\upsilon \rightarrow A^{+} + e_{p} \tag{1}$$

Here, the resonant intermediate state A^{+} is referred as the initial state of the decay process and e_{p} is the primary emitted electron. In the case of x-ray processes the vacancy moves to an outer shell under emission of characteristic x-rays

$$A^{+} \rightarrow A^{+} + h\upsilon' \tag{2}$$

where $h\upsilon'$ is the characteristic x-ray.
If the inner-shell vacancy is filled via Auger process resulting in two vacancies

$$A^{+} \rightarrow A^{2+} + e_{Auger} \tag{3}$$

The calculation of final charge state distributions and average number of ejected electrons following de-excitation decay of inner-shell vacancies has been carried out by the Monte-Carlo algorithms. This method is based on the simulation of all possible radiative and non-radiative pathways to fill the inner-shell vacancies in atom. The detailed description of the Monte-Carlo method has been given by El-Shemi et al. [20] and Abdullah et al. [21].

The radiative, non-radiative transitions and electron shake off processes are the principle mechanisms of a cascade originating from an inner- shell vacancy in atoms. The electron shake off process caused by the change of atomic potential is due to the creation of core hole and the decay through radiative and non-radiative transitions. The radiative branching ratios (fluorescence yields) and non-radiative branching ratios (Auger yields) give valuable information on the de-excitation dynamic of an atom with an inner-shell vacancy, are calculated. The radiative branching ratios (fluorescence yields) ω is defined as the probability that the vacancy in an initial state *i* is filled through radiative transitions under the emission of characteristic x-ray from final state *f*, and is given by:

$$\omega = \frac{A(if)}{A(i) + A(a)} \tag{4}$$

where $A(if)$ is the radiative transition rate from initial state i to final state *f*, $A(i)$ is the total radiative decay rate of state *i*, and $A(a) = \sum_f A(a_{if})$ is the total Auger and Coster-Kronig decay rate of final state *f*. The non-radiative branching ratios (*a*) are defined as the probability that the vacancy in an initial state *i* is filled through radiative transitions under emission of electrons state *f*, and is given by:

$$a = \frac{A(a_{if})}{A(i) + A(a)} \tag{5}$$

The radiative transition rates $A(if)$ for singly ionized atoms are calculated using Multiconfiguration Dirac Fock (MCDF) wave functions from Grant et al. [22]. The non-radiative transition rates $A(a_{if})$ for single ionized atoms are calculated using the Dirac Fock Slater wave functions using a code written by Lorenz and Hertmann [23].

The electron shake off process due to sudden change of atomic potential during vacancy cascade development leads to the ejection of additional electrons through monopole processes, this process is calculated using a code developed by El-Shemi [24]. The electron shake off probabilities are calculated by overlapping integrals between the wave functions of initial state φ_i and the final state φ_f of the transition process $\mathring{A}berg$ [25, 26]. So the probability of an electron transition from the orbital nlj to the orbital $n'l'j'$ is given by

$$p_{nlj \to n'l'j'} = \left| \int \varphi^*_{nlj}(A_0) \varphi_{n'l'j'}(A) d\tau \right|^2 \tag{6}$$

where $\varphi_{nlj}(A)$ and $\varphi_{n'l'j'}(A_0)$ are orbital wave functions for the orbital nlj and for the orbital $n'l'j'$ in the ion A_0. The probability that at least one of the N electrons located in the sub–shall nlj becomes ionized is given by

$$p = 1-(\left|\int \varphi^{*}_{nlj}(A_0)\varphi_{n'l'j'}(A)d\tau\right|^2)^N - p_f \qquad (7)$$

where the quantity P_f represents a correction factor for transitions to occupied shells (not allowed transitions) and has the form

$$p_f = \sum_{n'lj} N\frac{N'}{2j+1}\left|\int \varphi^{*}_{n'lj}(A_0)\varphi_{nlj}(A)d\tau\right|^2 \qquad (8)$$

with $n' \neq n$ and N' is the number of the electrons in the orbital $n'lj$.

An analysis of each cascade begins with the considration of all possible electron transitions which may fill an initial vacancy. In the following development of the cascade in each step, the computer program selects one of the possible processes according to their relative probabilities by the use of random numbers. After realization of the selected transition, a new configuration of vacancies appears. For each vacancy, first determine whether electron shake off will take place or not, using the total shake off probability for that shell. If an electron shake off take place, the atomic shell, from which the shake off electron is ejected, is determined according to relative shake off probabilities and the number of vacancies is increased by one. In the next step, the program decides from the fluorescence yield whether the transition is radiative or non-radiative transition. When it is radiative, the new position of the vacancy is selected from the partial radiative transition probabilities. In the case of Auger and Coster-Kronig transitions, two new vacancies are generated according to the relative transition probabilities of the energetically allowed Auger channels. The creation of multiple vacancies in atomic configurations during vacancy population causes transition energy shifts and may result in an energetic closing of channel for certain Coster-Kronig transitions. In the determination of the population of the multiple vacancy states, the vacancy cascade modeling takes into account the fact that the change of radiative and non- radiative transition rates due to transition energy shifts. The correction of the transition rates quantum mechanically requires more complex calculations. Therefore the transition rates were calculated according to the following scheme. At first quantum mechanically determined transition rates were calculated for single ionized atoms. The corrected transition rates for multi-ionized atoms have configuration with more vacancies are calculated using the scaling procedure proposed by Larkins [27]. So, the corrected radiative and non-radiative transition rates during vacancy cascade development are obtained using the scaling procedure as following:

For radiative

$$\Gamma_r = n_1 \frac{(N_2 - n_2)}{N_2} \Gamma_R \tag{9}$$

where n_1 and n_2 are the vacancies in initial and final states respectively. N_2 is the occupation numbers for the final state f.

For non-radiative

$$\Gamma_a = \frac{N_1 N_2}{(4l_1 + 2)(4l_2 + 2)} \Gamma_A \qquad \text{for non-equivalent electrons} \tag{10}$$

and

$$\Gamma_a = \frac{N_1 (N_1 - 1)}{(4l_1 + 2)(4l_1 + 2 - 1)} \Gamma_A \qquad \text{for equivalent electrons} \tag{11}$$

where N_1 and N_2 are the occupation numbers for the final state f and l_1 and l_2 are the orbital quantum numbers. Γ_a are the non-radiative transition rates for multi-ionized atoms and Γ_A for single ionized atoms.

For each new vacancy the computer program goes back to the first step described above. The appearance of new vacancy configurations continues untill all these vacancies reach the outer shell. Then the number of vacancies are recorded. After finishing with one cascade, the same initial vacancy will again be created in the inner-shell and the cascade will be again simulated. The probabilities of charged ions state distributions $p(Z_f)$ and the average charged ions $\langle Z_f \rangle$ are recorded after 10^5 histories. After 10^5 histories a stable final charge state distributions $p(Z_f)$ and the mean charged ions $\langle Z_f \rangle$ are produced.

$$\langle Z_f \rangle = \sum_n n \; p(Z_f) \tag{12}$$

where n is the degree of ionization.

3. Results and Discussions:

The final Charge state of ions formed after $1s \rightarrow \infty$ photoionization in Ne atom are illustrated in Fig. (1). The photoionization create 1s vacancy as one electron removes into continuum $1s \rightarrow C$, in this case the electronic configuration of single ionized neon atoms is given as $1s^{1+}_{1/2} 2s^{2}_{1/2} 2p^{2}_{1/2} 2p^{4}_{2/3}$. The charge state distributions produced by the vacancy cascades following from $1s \rightarrow \infty$ vacancy, in this case the *1s* core hole created by photoionization energy is above the ionization threshold of the *K* shell. In the *1s* vacancy situation, the decay lead to probabilities of final charge Ne^{1+}*=1%,* N^{2+}*=78%,* N^{3+}*=21%* and Ne^{4+}*=0.09* respectively. The Ne *1s* ionization mainly yields doubly charged ions via non-radiative *K-L*$_1$*L*$_1$*, K-L*$_1$*L*$_2$*, K-L*$_1$*L*$_3$*, K-L*$_2$*L*$_2$*, K-L*$_2$*L*$_3$ and *K-L*$_3$*L*$_3$ Auger transitions. The low intensity of Ne^{1+} ions produced following the decay of *1s* through $K\alpha$ radiative (x-ray) transitions, which occur in 0.7% of the cases as given by fluorescence yield. In this path, a *2p* electron fills a *1s* hole and a x-ray is emitted. According to the selection rules for dipole transitions the $1s \rightarrow$ 2p is the only allowed transition. The probability of filling *1s* hole through Auger transitions is 99.3% according to non-radiative yield. The (*2s*,*2s*), (*2s*,*2p*) and (*2p*,*2p*) Auger transitions are possible for filling the *K* shell vacancy in neon. These transitions lead to double charged Ne^{2+} ions. The radiative and non-radiative transitions are not permitted in the *2p* hole situation in Ne, so the Ne^{3+}, Ne^{4+} ions produce from Double Auger processes and electron shake off process. The number of ejected electrons $< Z_f >$ yields after $1s \rightarrow \infty$ photoionization is equal 2.3.

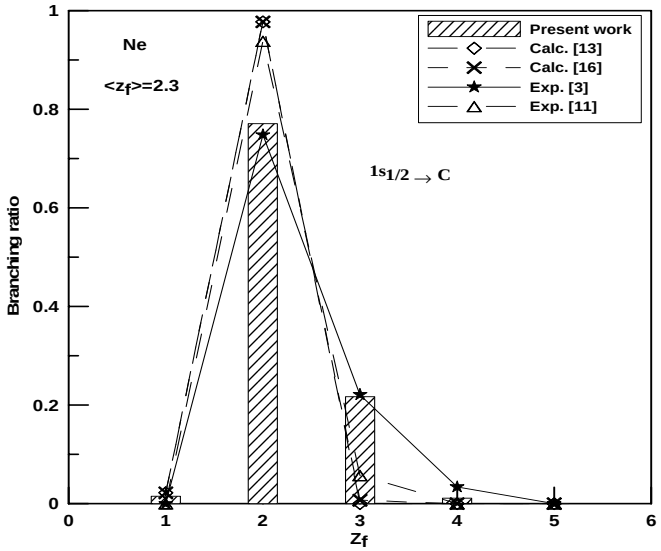

Fig. (1): Final charge state distributions following photoioniztion$1s \rightarrow \infty$ in neon atom. The average number of ejected electrons are given in the left corner.

Figure (2). shows the charge state distributions following resonant excitation $1s \rightarrow 3p$ in neon atom. The emission of one electron from *K*-shell to bound state *3p* as resonant excitation produced the following electronic configuration $1s^{1+}_{1/2} 2s^{2}_{1/2} 2p^{2}_{1/2} 2p^{4}_{2/3} 3p$. The final charge state after Ne *1s* resonant excitation ($1s \rightarrow 3p$) gives rise to Ne^{1+}, Ne^{2+} and Ne^{3+} with the probabilities in percent *P(Ne^{1+}) =56%, P(Ne^{2+}) = 43%* and *P(Ne^{3+}) = 1%.* The average number of ejected electrons $< Z_f >$ after $1s \rightarrow 3p$ resonant excitation is equal 1.97. The results of final charge state distributions after photoionization ($1s \rightarrow C$) are compared with theoretical and experimental values, but the results produced after resonant excitation ($1s \rightarrow$ 3p) are compared with available theoretical values.

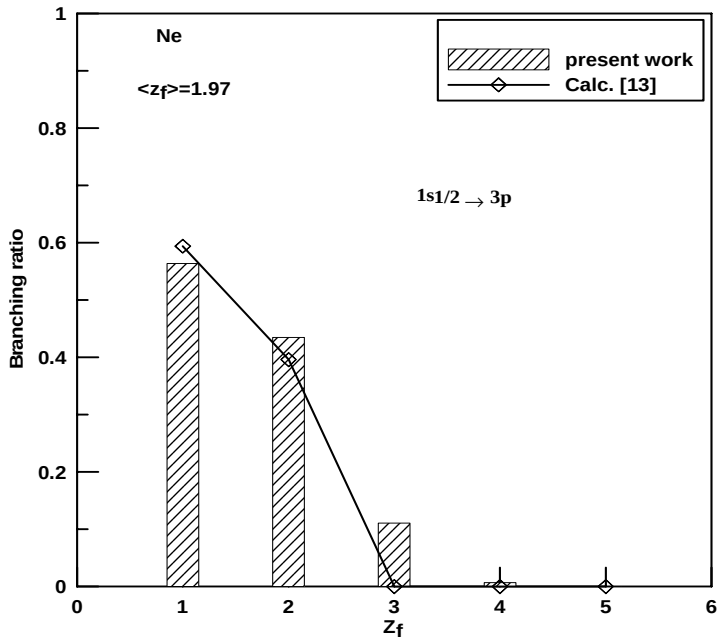

Fig. (2): The final charge state distributions after excited resonant 1s-3p in neon. The average number of ejected electrons are given in left corner.

The highly charged ions formed after photoionization $2s \rightarrow \infty$ and resonant excitation $2s \rightarrow 3p$ in neon atoms are illustrated in Fig. (3) and 4. The photoionization create *2s* vacancy as one electron removes into continuum ∞, while the resonant excitation produce *2s* vacancy as one electron removes into empty bound excited state *3p*. The electronic configuration after

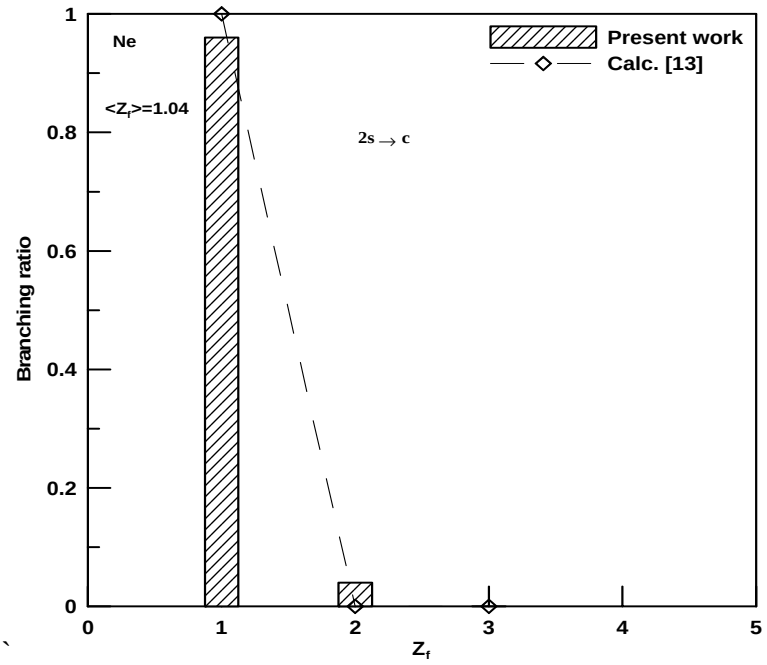

Fig. (3): Final charge state distributions after photoionization $1s \rightarrow \infty$ in neon atoms. The average number of ejected electrons is given in the left corner.

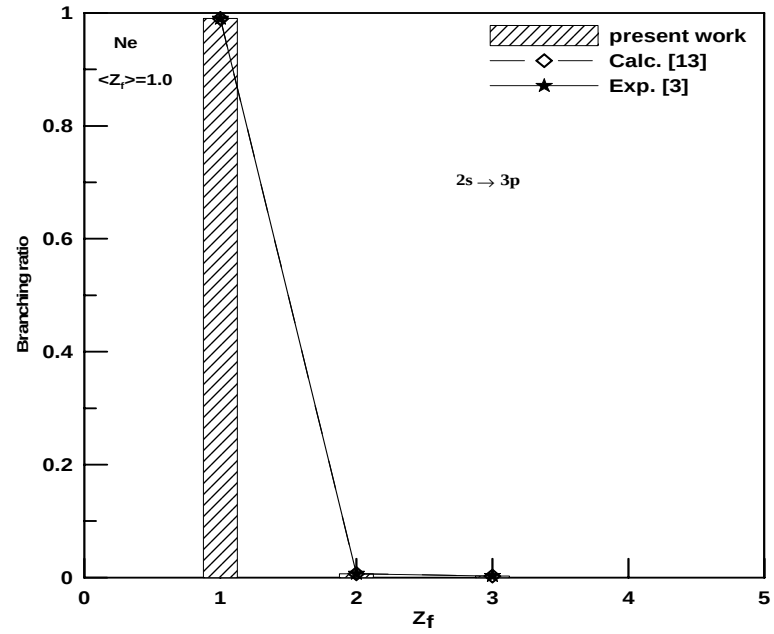

Fig. (4): Final charge state distributions after resonant excitation $2s \rightarrow 3p$ in neon atoms. The average number of ejected electrons is given in the left corner**.**

photoionization $2s \rightarrow \infty$ is written as $1s^2_{1/2} 2s^{1+}_{1/2} 2p^2_{1/2} 2p^4_{2/3}$ (as one vacancy created in L_1). The emission of one electron from *2s* into empty bound excited state *3p* leads to the atomic configuration $1s^2_{1/2} 2s^{1+}_{1/2} 2p^2_{1/2} 2p^4_{2/3} 3p$. The final charge state after Ne *2s* photoionization ($2s \rightarrow C$) gives rise to Ne^{1+}, Ne^{2+} with the probabilities in percent *P(Ne^{1+}) =96%, P(Ne^{2+}) =4%.* The radiative and non-radiative transitions are not permitted in the *2s* hole situation in Ne. The Ne^{2+} ions yield from electron shake off process. The singly charged ions Ne^{1+} are predominate after *2s* resonant excitation in Ne atoms. The electron shake off probabilities not appears in the *2s* resonant excitation situation.

4. Conclusion:

The final charge state distributions after $1s \rightarrow \infty$ and $2s \rightarrow \infty$ photoionization and $1s \rightarrow 3p$ and $2s \rightarrow 3p$ resonant excitation in Ne atoms are calculated. The calculation method based on the simulation of possible de-excitation pathways including radiative and non-radiative transitions to fill the vacancies produced in atomic shell configurations and electron shake off processes, which is due to the change of atomic potential after primary hole production. The radiative transition probabilities (x-ray transitions) are calculated for single ionized atom and multi-ionized atom using a Multiconfiguration Dirac Fock (MCDF) wave functions. The non-radiative transitions (Auger transitions) are calculated using Dirac Fock Slater (DFS) wave functions. The charged ions at 1s hole state after photoionization mainly turns into Ne^{2+} and Ne^{3+} ions. The production of Ne^{2+} ions is dominant after photoionization, while after resonant excitation mainly turns into Ne^{1+}. At *2s* hole state after photoionization and resonant excitation, the charged Ne^{1+} is predominate in the distributions. The results of charge state distributions of ions after core hole production agree well with the experimental values.

References:

1. D. A. Church , S. D. Kravis, I. A. Sellin, C. S. O. J. C. Levin, R. T. Short, M. Meron, B. M. Johnson, and K. W. Jones; *Phys. Rev*. A **36** (1987) 2487.

2. K. Ueda, E. Shigemasa, Y. Sato, A. Yagashita, T. Sasaki and T. Hayaishi; *Rev. Sci. Instrum*., **60** (1989) 2193.

3. M. O. Krause, M. V. Vestal, W. H. Johnson, T. A. Carlson; *Phys. Rev*., **133,** (1964), 385-90.

4. T.A. Carlson and M.O. Krause; *Phys. Rev*., A **137**, (1965),1655.

5. M. O. Krause and T. A Carlson; *Phys. Rev*., A **158**, (1967) 18

6. T.A. Carlson and M.O. Krause; *Phys. Rev. Letters,* **14**,(1965), 390.
7. T.A. Carlson, W. E. Hunt, and M.O. Krause; *Phys. Rev*., A **151**, (1966), 41-47.
8. T.A. Carlson and M.O. Krause; *Phys. Rev*., A **137**, (1965), 1655-1662.
9. T. Hayaishi, Y. Morioka, Y. Kageyama, M. Watanabe, I. H. Suzuki, A. Mikuni, G. Isoyama, S. Asaoka and M. Nakamura; *J. Phys. B: At. Mol. Phys*., **20**, (1987), L287.
10. T. Mukoyama, T. Tonuma, A. Yagishita, H. Shibata, T. Matsuo, K. Shima and H.
11. Tawara; *J. Phys. B: At. Mol. Phys*.,**20,** (1987), 4453.
12. N. Saito and I. H. Suzuki; *J. Phys. B: At. Mol. Opt. Phys*., **25**, (1992), 1785.
13. H. Tawara, T. Hayaishi, T. Koizumi, T. Matsuo, K. Shima ,T.Tonuma and A. Yagishita; *J. Phys. B* **25**, (1992), 1476-1473.
14. G. Omar and Y. Hahn; *Phys. Rev. A,* **43**, (1991), 4695.
15. G. Omar and Y. Hahn; *Phys. Rev. A,* **44**, (1991), 483.
16. A. G. Kochur, A. I. Dudenko, V. L. Sukhorukov and I. D. Petrov; *J. Phys. B: At. Mol. Opt.,* **27**, (1994), 1709.
17. G. Kochur, V. L. Sukhorukov, A. I. Dudenko and P.V.Demekhin, *J. Phys. B* **28**, (1995), 387-402.
18. T. Mukoyama; *Bull. Inst. Chem. Res. Kyoto Univ*., **63**, (1985), 373.
19. N. Mirakhmedov and E. S. Parilis; *J. Phys. B: At. Mol. Opt. Phys*.,21,(1988),795.
20. M. G. Opendak; *Astrophysics and Space Science* **165** (1990) 9
21. A. M. El-Shemi, A. A. Ghoneim and Y. A. Lotfy; *Turk. J. Phys*., **27**, (2003), 51.
22. H. Abdullah, A. M. El-Shemi and A. A. Ghoneim; *Rad. Phys. and Chem*., **68**, (2003), 697.
23. I. P. Grant, B. J. Mckenzie, P. Norrington, D. F. Mayers and N. C. Pyper; *Comput. Phys. Commun*. **21,** (1980), 207.
24. M. Lorenz, E. Hartmann; *Report ZFI-109*, Leipzig (1985) 27.
25. A. El- Shemi; *Egypt. J. Phys. 27, No. 1-2pp*. (1996) 231.
26. T. Aberg; *Phys. Rev*. 156 (1967) 35.
27. T Aberg; *Ann. Acad. Sci. Finn. Ser. AVI Phys*. 308 (1969) 7.
28. F. P. Larkins; *J. Phys. B: At. Mol. Phys*. **4** (1971) L29